



**HAL**  
open science

# Hybrid Vehicle Energy Management: Singular Optimal Control

Sebastien Delprat, Theo Hofman, Sebastien Paganelli

► **To cite this version:**

Sebastien Delprat, Theo Hofman, Sebastien Paganelli. Hybrid Vehicle Energy Management: Singular Optimal Control. IEEE Transactions on Vehicular Technology, 2017, 66 (11), pp.9654-9666. 10.1109/TVT.2017.2746181 . hal-03429438

**HAL Id: hal-03429438**

**<https://uphf.hal.science/hal-03429438v1>**

Submitted on 30 Sep 2024

**HAL** is a multi-disciplinary open access archive for the deposit and dissemination of scientific research documents, whether they are published or not. The documents may come from teaching and research institutions in France or abroad, or from public or private research centers.

L'archive ouverte pluridisciplinaire **HAL**, est destinée au dépôt et à la diffusion de documents scientifiques de niveau recherche, publiés ou non, émanant des établissements d'enseignement et de recherche français ou étrangers, des laboratoires publics ou privés.

# Hybrid Vehicle Energy Management: Singular Optimal Control

Sébastien Delprat<sup>1b</sup>, Theo Hofman<sup>1b</sup>, and Sébastien Paganelli

**Abstract**—Hybrid vehicle energy management is often studied in simulation as an optimal control problem. Under strict convexity assumptions, a solution can be developed using Pontryagin’s minimum principle. In practice, however, many engineers do not formally check these assumptions resulting in the possible occurrence of so-called unexplained “numerical issues.” This paper intends to explain and solve these issues. Due to the binary controlled-state variable considered (e.g., switching on/off an internal combustion engine) and the use of a lookup table with linear interpolation (e.g., engine fuel consumption map), the corresponding Hamiltonian function can have multiple minima. Optimal control is not unique. Moreover, it is defined as being singular. Consequently, an infinite number of optimal state trajectories can be obtained. In this paper, a control law is proposed to easily construct a few of them.

**Index Terms**—Binary variable, hybrid vehicle, lookup table, optimal control, singular control.

## I. INTRODUCTION

ENERGY management of hybrid vehicles has been studied intensively over the past two decades. Several approaches have been investigated for offline optimization, especially Pontryagin’s Minimum Principle (PMP). In this context, the optimal control algorithm is used to compute a state trajectory with endpoint constraints. This theory has some limiting theoretical requirements; in particular, the Hamiltonian associated with the optimal control problem must be convex and smooth [1]. Many engineers may stretch these theoretical limitations to solve different practical problems by using, in the models, lookup tables with linear interpolation and/or (heuristic) rules in order to include binary switching components in the control. Pontryagin’s Minimum Principle generally provides satisfactory solutions. However, so-called “numerical issues” are sometimes encountered and remain unexplained and unsolved.

This work was supported in part by the Regional Delegation for Research and Technology, in part by the French Ministry of Higher Education and Research, in part by the National Center for Scientific Research, and in part by the ELSAT2020 Project, cofunded by the European Regional Development Fund, the French state, and the Hauts de France Region Council. The review of this paper was coordinated by Dr. M. Kazerani. (*Corresponding author: Sébastien Delprat.*)

S. Delprat and S. Paganelli are with the LAMIH UMR CNRS 8201, University of Valenciennes and Hainaut Cambrésis, Le Mont Houy, Valenciennes 59313, France (e-mail: sebastien.delprat@univ-valenciennes.fr; sebastien.paganelli@univ-valenciennes.fr).

T. Hofman is with the Department of Mechanical Engineering, Eindhoven University of Technology, Eindhoven 5600 MB, The Netherlands (e-mail: t.hofman@tue.nl).

One of the most common issues is that the final end-point constraint cannot be satisfied by the optimal control algorithm.

The work presented intends to provide theoretical explanations and rigorous solutions to these “numerical issues” (e.g., solutions that ensure the optimality conditions for problems with linear interpolation and binary value optimization are satisfied).

The paper is organized as follows. In Section II, the optimal energy management of a parallel hybrid vehicle is introduced and the “numerical issues” studied are highlighted in different driving cycles. In Section III, a simple series hybrid vehicle model is detailed (no mechanical connection between the engine and the driven wheels). The fuel consumption to be minimized is computed using a lookup table with a linear interpolation. The power delivered by the Auxiliary Power Unit (APU) and its on/off signal are controlled. The hybrid vehicle energy management is formulated as an optimal control problem, and the classical implementation of Pontryagin’s Minimum Principle is recalled. Control is obtained by minimizing the Hamiltonian associated with the optimal control problem. The optimization problem comes down to the choice of a single parameter: the initial co-state value. This boundary value problem described by a nonlinear function is solved numerically. The resulting algorithm is applied to the energy management problem presented and the numerical issues are highlighted.

In Section IV, a rigorous optimal control algorithm is derived from Pontryagin’s Minimum Principle. The Hamiltonian minimization explicitly accounts for the binary variable (through relaxation) and the piecewise linear model resulting from the lookup table. The Hamiltonian is neither smooth nor strictly convex. For some specific co-state values, it has an infinite number of minima and the control is said to be singular. The effect of singular control on the state dynamics is illustrated. For given co-state values, an infinite number of state trajectories can be obtained and so an infinite number of final state values can be reached. Finally, a new PMP-based algorithm for singular control problems is introduced that allows a few optimal state trajectories to be obtained in the case of singular control. In Section V, the proposed algorithm is applied to both the series hybrid vehicle and the parallel hybrid vehicle studied. The computational performances of the proposed algorithm are discussed. From both the theoretical study and numerical simulations, the main factors causing the numerical issues are highlighted. Some explanations and recommendations are then formulated to facilitate the implementation of optimal hybrid vehicle energy management. Finally, some conclusions and perspectives are discussed in Section VI.

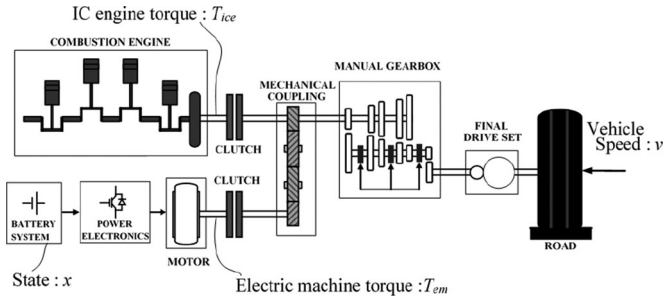


Fig. 1. Parallel single shaft hybrid powertrain considered.

TABLE I  
MODEL PARAMETERS

Description	Value
Vehicle Mass	1216 kg
Engine power	74 kW
Drag coefficient	0.36
Tire Rolling resistance coefficient	0.01
Nominal battery voltage	231 V
Battery capacity	10 Ah
Electric machine power	20 kW

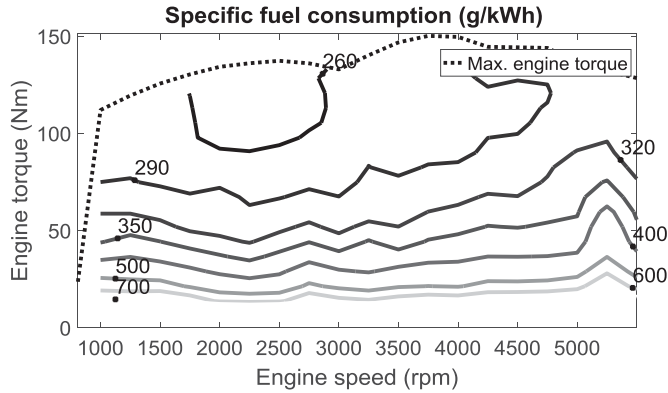


Fig. 2. IC engine specific fuel consumption.

## II. PROBLEM STATEMENT

Before analyzing the mathematics behind singular control in a simpler problem, let us introduce the following use case. A parallel single shaft hybrid vehicle, composed of an internal combustion engine coupled to a battery-powered electric machine via a mechanical transmission, is considered, Fig. 1. Two clutches are used to disconnect the motor and/or the engine. The power is transferred to the wheel through a five-gear manual transmission and a differential. The vehicle parameters are listed in Table I.

Hybrid vehicle simulations for energy studies can be implemented in various ways: Simulink-based models in the Advisor software [2] or MATLAB scripts as is used in this work. The IC engine specific fuel consumption map and the electric machine efficiency map are given in the Figs. 2 and 3.

In this study, the New European Driving Cycle and some driving cycles from the HYZEM project are considered, Fig. 4. To cope with two energy sources, one of the simplest approaches is

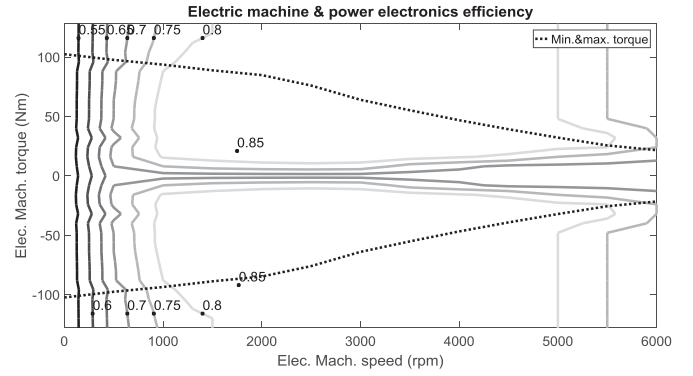


Fig. 3. Electric machine & power electronics efficiency.

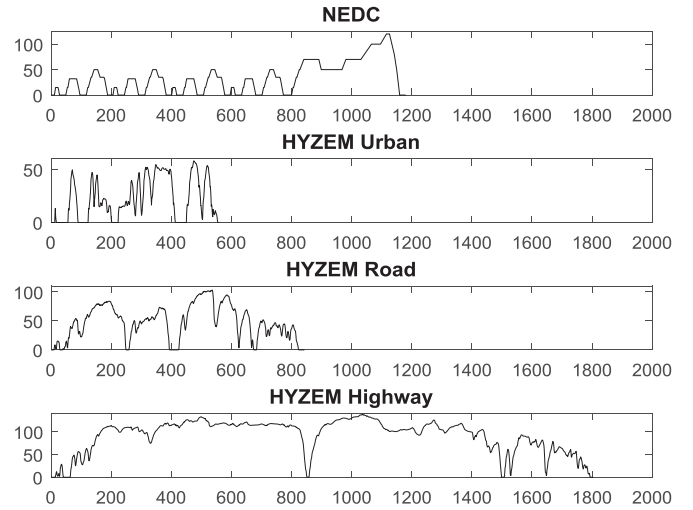


Fig. 4. Velocity profile (in km/h) of the driving cycles considered

to impose, over a driving cycle, identical initial and final battery states of charge. The hybrid vehicle energetic performance is there reduced to the fuel consumption.

In this work, the focus is on Pontryagin's Minimum Principle, which has been studied intensively over the last decade [3], [4]. The algorithm implemented is quite common and is described in [5], [6]. The objective is to compute the torque split between the engine and the electric machine to minimize the fuel consumption while imposing the final battery state of charge, denoted as  $x_T$ . For the simulation presented, the initial and final states of charge were set to  $x_0 = 50\%$  and  $x_T = 50\%$ .

The algorithm is unable to compute a solution that matches the final state of charge constraint. Therefore, the nearest two solutions with a final state of charge upper and lower to the requested one are returned. The first solution had a fuel consumption of 3.60 l/100 km and a final state of charge error of 0.42% vs 3.5 l/100 km and  $-1.06\%$  for the second one.

Several simulations were performed with the considered driving cycles to numerically estimate the highest final state of charge error. The fuel consumption uncertainty is defined as the possible variation of the fuel consumption between both solutions. The results are summarized in Table II. For the NEDC, the maximum final state error can be as large as 12.2%, Fig. 5.

TABLE II  
WORST CASE SIMULATION CONDITIONS FOR DIFFERENT DRIVING CYCLES

	NEDC	HYZEM		
		Urban	Road	Highway
Initial state of charge $x_0$ (%)	50	50	50	100
Expected final state of charge $x_T$ (%)	67.15	60.45	70.25	6.62
Final state of charge error $x(T) - x_T$ (%)	<b>12.15</b>	<b>0.14</b>	<b>-0.92</b>	<b>0.60</b>
Sol no. 1 fuel consumption (l/100 km)	5.66	5.17	4.51	4.46
Sol no. 2 fuel consumption (l/100 km)	3.94	5.11	4.38	4.44
Fuel consumption uncertainty (%)	<b>30.38</b>	<b>1.22</b>	<b>2.69</b>	<b>0.40</b>

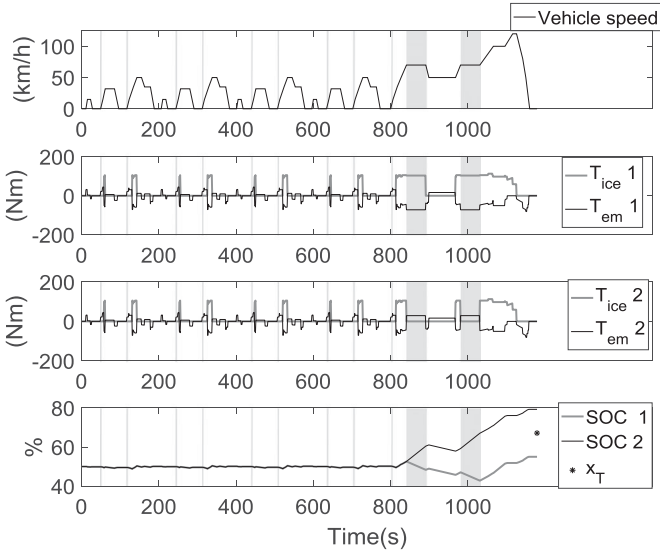


Fig. 5. Worst case final state of charge error over the NEDC. Grayed areas highlight differences between the solutions.

Several issues are related to the final state of charge errors and fuel consumption uncertainty encountered. (i) During the design phases, the analysis of the vehicle energetic performance must take into account the energy related to the final state error (through a SOC correction routine for instance) and/or possible fuel consumption variation. (ii) The optimal control algorithm is likely to use additional computation time trying to cancel the final state of charge error. The computational performance can be an issue: the optimal control algorithm can be embedded in a real time predictive framework [7] with limited CPU power. Hybrid vehicle sizing algorithms compute solutions for numerous driving cycles and hundreds of vehicle sizes [6], therefore unnecessary iterations increases the computation time. (iii) The theory behind the optimal control algorithm states that the final state error can be efficiently canceled. So *apparently*, there is a mismatch between theory and practice.

As it will be demonstrated, most of the optimal hybrid vehicle energy management algorithms that include (explicitly or not) binary variable optimization are *theoretically* incorrect (even if acceptable results may be obtained in practice). The main

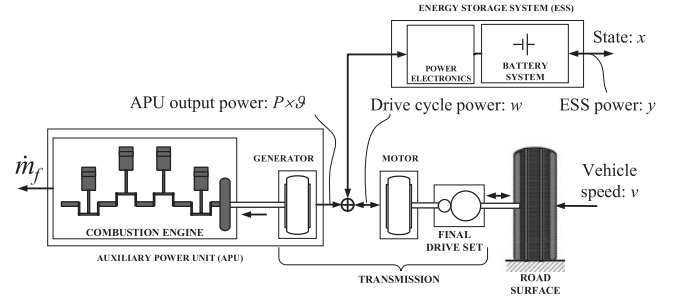


Fig. 6. Series hybrid powertrain considered.

contribution of this work is an algorithm built on theoretical foundations that solves the final state errors experienced.

### III. HYBRID VEHICLE ENERGY MANAGEMENT

In order to simplify the mathematical expressions, a series hybrid vehicle is preferred to the parallel hybrid architecture. The algorithm proposed can be easily adapted to other arrangements (such as a parallel hybrid powertrain) with a single degree of freedom.

The vehicle considered (depicted in Fig. 6) is composed of an electric vehicle powered by an Auxiliary Power Unit (APU) and/or an Energy Storage System (ESS).

In simulation, a driving cycle provides the vehicle speed as a function of time  $t$ . The vehicle energy consumption is accurately described by quasi-static models for the engine, the electric machines, and the battery system [8], [9]. The principal vehicle parameters are listed in Table VII of Appendix.

#### A. System Description: Series Hybrid Powertrain

The auxiliary power unit output power  $P(t)$  was chosen as the control variable. It is constrained by some physical limitations:

$$P(t) \in [0, P^{\max}] \quad (1)$$

In order to lighten the notations, the dependence on the time variable  $t$  is omitted when there is no ambiguity. In addition, let us denote  $\vartheta(t) \in \{0, 1\}$  as the primary energy source binary control (for instance, the fuel injection-enabling signal) with  $\vartheta(t) = 0 \Rightarrow P(t) = 0$ .

In many cases [4], [10], it is assumed that the driving cycle power  $w(t)$  is piecewise constant, where  $T_s$  is the sampling period and  $n_w$  is the number of samples:

$$w(t) = w_i \quad \forall t \in [i \cdot T_s, (i+1) \cdot T_s[ \quad i = 0, \dots, n_w - 1 \quad (2)$$

The energy storage system power is limited due to the electrical system component constraints:

$$y(t) \in [-y^{\max}, y^{\max}] \quad (3)$$

The hybrid power split is defined as:

$$\vartheta(t) \cdot P(t) = y(t) + w(t) \quad (4)$$

According to the limits of the different components (1), (4) and the driving cycle power  $w(t)$ , the binary control variable may be limited or not. Let us denote  $\vartheta(t) \in \Phi(w(t))$  with

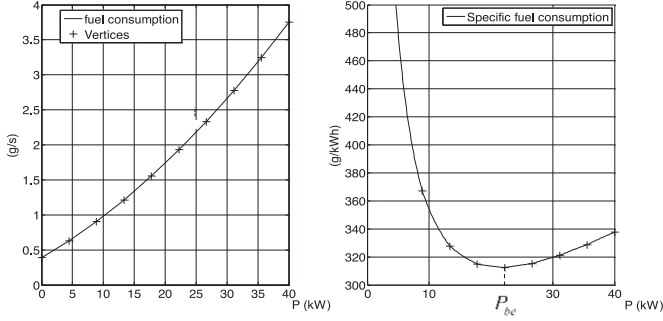


Fig. 7. Fuel consumption (g/s) and specific fuel consumption (g/kWh) as a function of the auxiliary power unit power  $P$ .

$\Phi(w) \subset \{\{0\}, \{1\}, \{0, 1\}\}$  as the set of admissible binary variable values with respect to  $w$ . The continuous control signal  $P(t)$  must be limited:

$$P(t) \in [\underline{P}(w(t)), \bar{P}(w(t))] \quad (5)$$

with  $\underline{P}(w(t)) = \max(0, -y^{\max} + w(t))$  and  $\bar{P}(w(t)) = \min(P^{\max}, y^{\max} + w(t))$

Let  $u(t) = [P(t) \vartheta(t)]^T \in U(w(t))$  be the decision variable with  $U(w(t)) = [\underline{P}(w(t)), \bar{P}(w(t))] \times \Phi(w(t))$  as the admissible control space at time  $t$ .

The energy storage system is considered as a dynamic system with  $x(t)$  being the state of energy. The main objective of this work is to study the effects of singular control, and so perfect energy storage is considered, as in [11], [12]. The storage capacity is denoted  $Q$ . The system dynamics is:

$$\dot{x}(t) = y(t) = (P(t) \cdot \vartheta(t) - w(t)) Q^{-1} \quad (6)$$

The fuel consumption is computed using a lookup table and linear interpolation between the gridded data points available (vertices), Fig. 7.

The  $n_P = 10$  lookup table breakpoints are denoted as  $p^j$ . The fuel consumption model is a piecewise linear function:

$$\dot{m}_f(P) = c_j \cdot P + d_j \quad \forall P \in [p_j, p_{j+1}[ \quad j = 0, \dots, n_P - 2 \quad (7)$$

Coefficients  $c_j$  and  $d_j$  are chosen such that  $\dot{m}_f$  is convex and continuous with  $c_0 > 0$ ,  $c_{j+1} > c_j$ ,  $d_0 > 0$ .

Fig. 7 also presents the specific fuel consumption of the auxiliary power unit. This corresponds to the ratio of the fuel-mass flow  $\dot{m}_f$  and the electric power  $P(t)$ . The best efficiency is achieved for  $P(t) = P_{be}$ :

$$P_{be} = \arg \min_{P \in [0, P^{\max}]} (\dot{m}_f(P) P^{-1}) \quad (8)$$

The auxiliary power unit fuel consumption over the driving cycle starting at  $t = 0$  and ending at time  $T$  is:

$$\min_{\substack{u(t) \in U(w(t)) \\ \forall t \in [0, T]}} J = \int_0^T \dot{m}_f(P(t)) \cdot \vartheta(t) \cdot dt \quad (9)$$

Two additional state constraints are needed [13], [14]:

$$x(0) = x_0 \quad (10)$$

$$x(T) = x_T \quad (11)$$

The optimal control problem considered, denoted *OCP*, is given by (4), (6), (9)–(11).

Several approaches such as convex programming [8], [15], [16] or deterministic Dynamic Programming (DP) [17], [18] have been investigated to solve the *OCP*. Pontryagin's Minimum Principle provides the necessary conditions for solution optimality enabling the initial optimization problem to be reduced to a boundary value problem. If the Hamiltonian is smooth and convex, this boundary value problem can be solved by a simple shooting algorithm [19]. PMP-based optimization algorithms are usually significantly faster than DP. However, state constraints are quite difficult to handle with Pontryagin's Minimum Principle [20]. Several iterative algorithms [21], [22], as well as penalty-based methods [23] have been proposed.

### B. Pontryagin's Minimum Principle

The work presented focuses on Pontryagin's Minimum Principle and is restricted to an unconstrained state problem for the sake of simplicity. By introducing the co-state  $\lambda(t) \in \mathbb{R}$ , the Hamiltonian of the optimization problem is:

$$H(w, u, \lambda) = S_\vartheta(P, \lambda) \cdot \vartheta - \lambda \cdot Q^{-1} \cdot w \quad (12)$$

with

$$S_\vartheta(P, \lambda) = \dot{m}_f(P) + \lambda \cdot Q^{-1} \cdot P \quad (13)$$

The following necessary first order optimality condition can be derived from Pontryagin's Minimum Principle [24], [25]:

$$\dot{\lambda}(t) = -\frac{\partial H}{\partial x} = 0 \quad (14)$$

This constant co-state is a well-known consequence of the chosen state-independent energy storage system model [4]:

$$\lambda(t) = \lambda_{\text{init}} \quad \forall t \in [0, T] \quad (15)$$

with  $\lambda_{\text{init}}$  as an unknown constant. The optimal control  $u(t)$  satisfies:

$$u(t) = \arg \min_{u(t) \in U(w(t))} H(w, u(t), \lambda_{\text{init}}) \quad (16)$$

The Hamiltonian minimization results in two functions of the exogenous variable  $w$  and the co-state value  $\lambda_{\text{init}}$ :

$$\left( \psi_P(w, \lambda_{\text{init}}) \psi_\vartheta(w, \lambda_{\text{init}}) \right)^T = \arg \min_{u \in U(w(t))} H(w, u, \lambda_{\text{init}}) \quad (17)$$

If the Hamiltonian is strictly convex with respect to the control  $u$ , the optimal solution is unique and conditions (14) and (16) are also sufficient.

The final state value is a function  $g$  of the initial co-state  $\lambda_{\text{init}}$ :

$$x(T) = g(\lambda_{\text{init}}) \quad (18)$$

$$g(\lambda_{\text{init}}) = x(0) + Q^{-1} \int_0^T (\psi_P(w, \lambda_{\text{init}}) \cdot \psi_\vartheta(w, \lambda_{\text{init}}) - w) \cdot dt \quad (19)$$

The only unknown is the initial co-state value,  $\lambda_{\text{init}}$ . It is computed numerically as a solution to:

$$g(\lambda_{\text{init}}) - x_T = 0 \quad (20)$$

### C. Classical Implementation of Pontryagin's Minimum Principle

In many studies, it is assumed that the Hamiltonian has a single minimum [10], [26], [27] and the Hamiltonian minimization is computed numerically. For instance, the set of admissible controls  $U(w(t))$  is replaced by a finite set of values denoted  $U_{\text{grid}}(w(t))$ . It is composed, for  $\vartheta = 1$ , of  $n_{\text{grid}}$  values linearly spaced within the admissible range of the continuous variable  $[\underline{P}(w(t)), \bar{P}(w(t))]$  and the pure electric mode (corresponding to  $\vartheta = 0$ ), if available. The Hamiltonian minimum is estimated by evaluating the Hamiltonian at each grid node [4], [10], and [28].

As a result, an approximate Hamiltonian minimization is obtained. Approximated values are denoted with a tilde. The optimal control (17) is replaced by:

$$(\tilde{\psi}_P(w, \lambda_{\text{init}}) \tilde{\psi}_\vartheta(w, \lambda_{\text{init}}))^T = \arg \min_{u \in U_{\text{grid}}(w)} H(w, u, \lambda_{\text{init}}) \quad (21)$$

The exogenous signal  $w$  being piecewise constant, the control should also be piecewise constant:

$$P(t) = \tilde{P}_i \quad \forall t \in [i \cdot T_s, (i+1) \cdot T_s[ \quad (22)$$

$$\vartheta(t) = \tilde{\vartheta}_i \quad \forall t \in [i \cdot s, (i+1) \cdot s[ \quad (23)$$

The values of  $\tilde{P}_i$  and  $\tilde{\vartheta}_i$  are obtained using the approximated control law:

$$\tilde{P}_i = \tilde{\psi}_P(w_i, \lambda_{\text{init}}) \quad (24)$$

$$\tilde{\vartheta}_i = \tilde{\psi}_\vartheta(w_i, \lambda_{\text{init}}) \quad (25)$$

The final state value is a function  $\tilde{g}$  of the initial co-state  $\lambda_{\text{init}}$ :

$$\tilde{g}(\lambda_{\text{init}}) = x_0 + Q^{-1} \sum_{i=0}^{n_w-1} \left( \tilde{\psi}_P(w_i, \lambda_{\text{init}}) \cdot \tilde{\psi}_\vartheta(w_i, \lambda_{\text{init}}) - w_i \right) \cdot T_s \quad (26)$$

The initial co-state value  $\lambda_{\text{init}}$  is the solution to the following equation:

$$\tilde{g}(\lambda_{\text{init}}) - x_T = 0 \quad (27)$$

A first numerical experiment was conducted with the New European Driving Cycle (NEDC). The numerical settings are

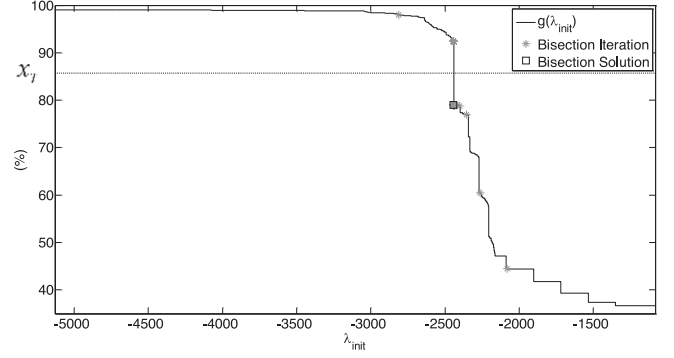


Fig. 8. Final state of energy as a function of the co-state for the NEDC.

TABLE III  
WORST CASE SIMULATION CONDITIONS FOR DIFFERENT DRIVING CYCLES OBTAINED WITH THE SERIES HYBRID VEHICLE

Driving cycle	Initial state of charge $x_0$ (%)	Expected final state of charge $x_T$ (%)	Final state of charge error $x(T) - x_T$ %
NEDC	50	85.67	-6.66
HYZEM Urban	50	63.18	-3.01
HYZEM Road	50	50.21	-2.16
HYZEM Highway	50	42.90	9.02

$x_0 = 50\%$ ,  $x_T = 85.67\%$  and  $n_{\text{grid}} = 100$ . The solution to (27) is computed using a bisection algorithm.

The function  $g(\lambda_{\text{init}})$  represented in Fig. 8, is subject to a number of discontinuities that may not allow a solution to (27) to be found. The bisection algorithm solution converges toward each side of the discontinuity. The solution closest to the desired final state of energy is retained when the algorithm is stopped. The initial co-state obtained is  $\lambda_{\text{init}} = -2442.5$ .

The fuel consumption is 12.71 l/100 km and the final state obtained is  $x(T) = 79.01\%$ , so the final state of charge error is  $x_T - x(T) = 6.66\%$ .

Worst case conditions were identified using simulations. The results are summarized in Table III. The maximum final state of charge error depends on the driving cycle and the requested initial/final state of charge. The worst case occurs with the HYZEM Highway driving cycle and not the NEDC. Without further analysis, these numerical results cannot be explained.

Theoretically, Pontryagin's Minimum Principle requires the control vector to be continuous. Additionally, if the Hamiltonian is convex with respect to the optimized variable, then the final state error can be made as small as necessary.

Using Pontryagin's Minimum Principle to optimize a binary variable requires additional analyses to solve the "numerical" errors encountered.

## IV. SINGULAR OPTIMAL CONTROL

To implement Pontryagin's Minimum Principle, it is first necessary to determine the control that minimizes the Hamiltonian. In order to fit the theoretical requirements of Pontryagin's Minimum Principle, the initial problem is replaced by an embedded problem similar to the *OCP*, except that  $\vartheta(t) \in [0, 1]$ . If the

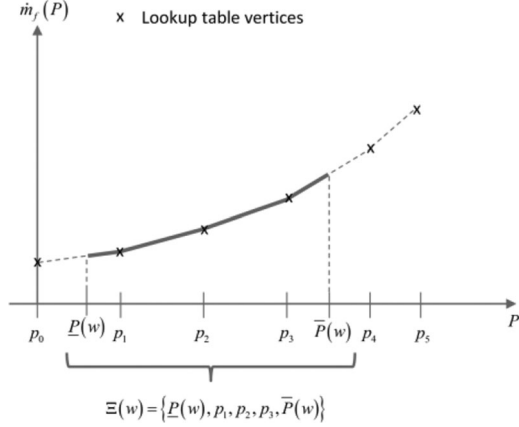


Fig. 9. Illustration of the admissible breakpoint set  $\Xi(w)$ . The solid line depicts the “useful” part of the auxiliary fuel consumption model,  $\forall P \in [P(w), \bar{P}(w)]$ .

solution to the embedded problem contains only  $\vartheta(t) \in \{0, 1\}$ , then it is also a solution of the initial optimization problem [29]. Moreover, in some particular situations the Hamiltonian has an infinite number of minima, therefore, the final state errors encountered with the classical algorithm can be rigorously explained.

Finally, an algorithm is proposed to construct an infinite number of optimal solutions with no final state error.

#### A. Hamiltonian Minimization

Two preliminary remarks need to be made.

First, the Hamiltonian can be formulated as a piecewise linear function of the power  $P$ :

$$H(w, u, \lambda) = [(c_j + \lambda Q^{-1}) \cdot P + d_j] \cdot \vartheta - \lambda \cdot Q^{-1} \cdot w \quad (28)$$

In the sequel, a piecewise expression is considered each time the coefficients  $c_j$  or  $d_j$  are used. It is assumed to be valid over the appropriate interval  $[p_j, p_{j+1}]$ .

Equation (28) can be rewritten to show that the Hamiltonian is a piecewise affine function of the single variable  $P$ , according to (29) where  $S_P$  is a so-called switching function defined by (30).

$$H(w, u, \lambda) = S_P(\lambda) \cdot P \cdot \vartheta + d_j \cdot \vartheta - \lambda \cdot Q^{-1} \cdot w \quad (29)$$

$$S_P(\lambda) = c_j + \lambda \cdot Q^{-1} \quad (30)$$

In a same way, the Hamiltonian is also a piecewise affine function of the single variable  $\vartheta$ , according to (31) where  $S_\vartheta$  is also a switching function.

$$H(w, u, \lambda) = S_\vartheta(\lambda, P) \cdot \vartheta - \lambda \cdot Q^{-1} \cdot w \quad (31)$$

$$S_\vartheta(P, \lambda) = c_j \cdot P + d_j + \lambda \cdot Q^{-1} \cdot P \quad (32)$$

Using the two switching function  $S_P$  and  $S_\vartheta$  will simplify the Hamiltonian behavior analysis.

The second remark is related to the control constraint (5). Only a small set of power values needs to be considered. As

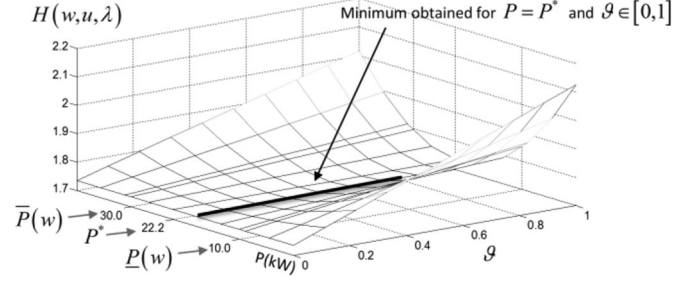


Fig. 10. The Hamiltonian as a function of the auxiliary power unit  $P$  and binary control  $\vartheta$  for  $w = 20$  kW and  $\lambda = \lambda_\vartheta(w) = -2155.44$ .

illustrated in Fig. 9, for any  $P \in [P(w), \bar{P}(w)]$ , this set, denoted as  $\Xi(w)$ , is composed of:

- 1) The admissible lookup table breakpoints with respect to the control constraint (5),
- 2) The minimum and maximum control values  $\{P(w), \bar{P}(w)\}$ .

The formal definition of the set  $\Xi(w)$  is:

$$\Xi(w) = \{p_j : p_j \in [P(w), \bar{P}(w)], j = 0 \dots n_P - 1\} \times \cup \{P(w), \bar{P}(w)\} \quad (33)$$

For a given  $w$  and  $\lambda_{init}$ , the optimal control law, denoted  $(P^*, \vartheta^*)$ , is obtained by minimizing the Hamiltonian. In general, there is a unique solution and the control is well defined. But, the Hamiltonian being piecewise affine, it may happen that for particular cases, the minimum is obtained for an infinite number of control variables. The control is then said to be singular. The sign of the two switching functions  $S_P$  and  $S_\vartheta$  determines if control singular or not, and different cases need to be considered.

The sign of the two switching functions  $S_P(\lambda)$  and  $S_\vartheta(P, \lambda)$  determines the control. If  $S_P(\lambda)$  or  $S_\vartheta(P, \lambda)$  is null for a non-null time interval, the control is singular and an additional analysis is required to compute a solution to the optimal control problem.

*Case 1*  $S_\vartheta(P^*, \lambda) = 0, \vartheta^* \in [0, 1]$ : In this case the binary variable is singular. For any co-state values such that  $S_\vartheta(P^*, \lambda) = 0$ , the Hamiltonian is a function similar to the one depicted in Fig. 10. Its minimum value is obtained for a particular value of the power  $P = P^*$ , but for an infinite number of values of the binary variable  $\vartheta \in [0, 1]$ , which is represented by the thick line.

For this set of points, the Hamiltonian is reduced to

$$H(w, (P^*, \vartheta)^T, \lambda) = -\lambda \cdot Q^{-1} \cdot w \quad (34)$$

If  $P^* = 0$  then  $S_\vartheta(0, \lambda) = d_0 > 0$ , which is excluded by the very definition of Case 1. Hence  $P^* > 0$  and the possible control and co-state values are a solution of  $S_\vartheta(P^*, \lambda) = 0$ :

$$\lambda = -\dot{m}_f(P^*) P^{*-1} Q \quad (35)$$

The co-state value is proportional to the opposite of the specific fuel consumption. Depending on the sign of  $w$ , minimizing the Hamiltonian (34) is equivalent to minimizing or maximizing the specific fuel consumption. Continuous control is obtained

by minimizing the Hamiltonian over the admissible control interval:

$$P^* = \arg \min_{P \in [\underline{P}(w), \bar{P}(w)]} (\dot{m}_f(P) P^{-1} Q w) \quad (36)$$

If  $w < 0$ , the solution of (36) is  $P^* = 0$  which is excluded in the present case. Hence  $w < 0$ .

Let us denote  $Sat(P, w)$  as the following saturation function:

$$Sat(P, w) = \max(\underline{P}(w), \min(P, \bar{P}(w))) \quad (37)$$

For any  $w > 0$ , the power that minimizes the Hamiltonian is:

$$P^* = sat(P_{be}, w) \quad (38)$$

Let us note that for a very efficient implementation of (38)  $P_{be} \in \{p_j\}_{j=0, \dots, n_P-1}$  and  $P^* \in \Xi(t)$ .

Due to the saturation in (38), different  $P^*$  are obtained for different values of  $w$ .

To summarize, the binary variable can be singular, i.e.,  $\vartheta^* \in [0, 1]$ , if  $w \geq 0$  and if the co-state takes the specific value:

$$\lambda_{\vartheta}(w) = -\dot{m}_f(sat(P_{be}, w)) (sat(P_{be}, w))^{-1} Q \quad (39)$$

As a result, for a given driving cycle, the co-state values  $\lambda_{\vartheta}(w)$  that lead to singular binary control can be computed easily using the exogenous variable samples  $w_i$ .

*Case 2:*  $S_{\vartheta}(P^*, \lambda) > 0$ ,  $\vartheta^* = 0$ : The binary variable  $\vartheta^*$  is equal to 0 and  $P^* = 0$ .  $S_{\vartheta}(P^*, \lambda) > 0$  holds for  $\lambda > \lambda_{\vartheta}(w)$ .

*Case 3:*  $S_{\vartheta}(P^*, \lambda) < 0$ ,  $\vartheta^* = 1$ :  $S_{\vartheta}(P^*, \lambda) < 0$  holds for  $\lambda < \lambda_{\vartheta}(w)$ . Let us first study the Hamiltonian minimization without control saturation. The optimal continuous variable  $P^*$  is a 'staircase-shaped' function dependent on the co-state  $\lambda$ :

$$P^* = \Psi(\lambda) \quad (40)$$

with

$$\begin{cases} \Psi(\lambda) = p_j & \text{if } \lambda > -Qc_j \\ \Psi(\lambda) = p_{j+1} & \text{if } \lambda < -Qc_j \\ \Psi(\lambda) \in [p_j, p_{j+1}] & \text{if } \lambda = -Qc_j \end{cases} \quad (41)$$

It is important to note that if  $\lambda = -Qc_j$  the control is singular: any value in  $[p_j, p_{j+1}]$  minimizes the Hamiltonian. This situation is depicted in Fig. 11 for  $\lambda = -Qc_5$  where  $P \in [p^5, p^6]$  minimizes the Hamiltonian.

In order to take saturation into account, (40) is replaced by:

$$P^* = sat(\Psi(\lambda), w) \quad (42)$$

To summarize the three cases, the optimal control law is actually composed of two multi-valued functions  $\psi_P(w, \lambda)$  and  $\psi_{\vartheta}(w, \lambda)$ :

$$\psi_P(w, \lambda) = \begin{cases} sat(\Psi(w, \lambda), w) & \text{if } \lambda < \lambda_{\vartheta}(w) \\ sat(P_{be}, w) & \text{if } \lambda = \lambda_{\vartheta}(w) \\ 0 & \text{if } \lambda > \lambda_{\vartheta}(w) \end{cases} \quad (43)$$

$$\psi_{\vartheta}(w, \lambda) = \begin{cases} 1 & \text{if } \lambda < \lambda_{\vartheta}(w) \\ [0, 1] & \text{if } \lambda = \lambda_{\vartheta}(w) \\ 0 & \text{if } \lambda > \lambda_{\vartheta}(w) \end{cases} \quad (44)$$

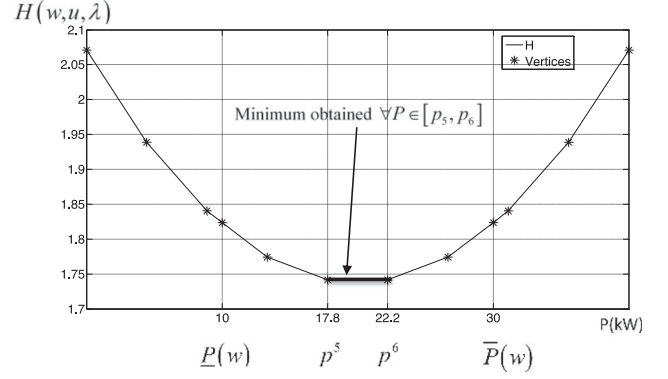


Fig. 11. Hamiltonian as a function of the auxiliary power unit power  $P$  for  $\lambda = -Qc_5 = -2087.53$  and  $w = 20$  kW.

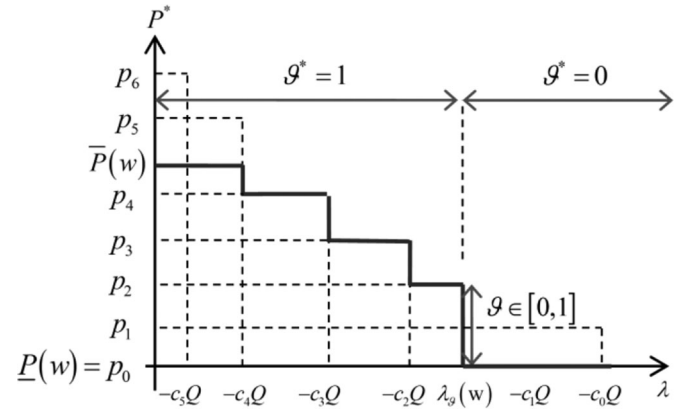


Fig. 12. Example of the Hamiltonian minimization results for  $w > 0$  and  $n_P = 7$ .

Continuous control is a staircase shaped function of the co-state until the co-state reaches the limit  $\lambda_{\vartheta}(w)$  and is null after. Due to control saturation, control may be regular despite the fact that  $\lambda = -Qc_j$  or  $\lambda = \lambda_{\vartheta}(w)$ . This is illustrated in Fig. 12 for  $\lambda = -Qc_5$ , where  $Sat(p_5, w) = Sat(p_6, w) = \bar{P}(w)$ .

The control value given by (43) inevitably belongs to the admissible breakpoint set  $\Xi(w)$  and can be computed without any additional interpolation. This allows very efficient implementation of the control law.

Let us now investigate the possible optimal state trajectories generated for a given initial co-state value.

### B. Effect of Singular Control on State Trajectories

As illustrated in Fig. 12, control is well defined for most of the co-state values and a finite number of final state values  $x(T)$  can be reached. These values correspond to the horizontal segments of the  $g$  function graph illustrated in Fig. 8.

Let us denote  $\Omega_{\vartheta}$  as the set of initial co-state values that generate at least a singular arc for the binary variable. This set is composed of all the possible values  $\lambda_{\vartheta}(w_i)$ , as defined by (39), evaluated for every  $w_i \geq 0$  over the entire driving cycle:

$$\Omega_{\vartheta} = \bigcup_{\substack{i \in \{0, \dots, n_w - 1\} \\ w_i \geq 0}} \{\lambda_{\vartheta}(w_i)\} \quad (45)$$

$\Omega_P$  denotes the set of initial co-state values that generate singular arcs for continuous control:

$$\Omega_P = \bigcup_{j=0}^{n_P-2} \{-Qc_j\} \quad (46)$$

Finally,  $\Omega$  is the set of initial co-state values that generate any singular arcs:

$$\Omega = \Omega_P \cup \Omega_\vartheta \quad (47)$$

The number of co-state values that generate trajectories with singular arcs is related to the driving cycle length  $n_w$  and the number of lookup table breakpoints  $n_P$  and cannot exceed  $n_w + n_P - 3$ . For the vehicle considered and the NEDC,  $n_w + n_P - 3 = 1232$ , but only 142 co-state values are used in practice due to duplicate driving cycle sample values and negative  $w_i$ .

If the problem has a solution for any  $\lambda_{\text{init}} \notin \Omega$ , the OCP is solved and the control is well defined over the entire driving cycle.

Let us assume that the final state value  $x_T$  requested cannot be reached using  $\lambda_{\text{init}} \notin \Omega$ . This is the case for almost all  $x_T$  values, which correspond to the vertical segments of the  $g$  function graph depicted in Fig. 8.

For a given  $x_T$ , the proper co-state value  $\lambda_{\text{init}}$  can be found using a bisection search algorithm within the ordered set  $\Omega$ . For this particular initial co-state value, the control is singular for one or more time intervals. Over these intervals, optimal control is not unique. A particular value of the final state is obtained by choosing a particular control value in the admissible range.

Let us denote  $I_s$  as the set of sample indices  $i$  such that  $\forall t \in [i \cdot T_s, (i+1) \cdot T_s[$  the binary or continuous control is singular, and  $I_r$  as the remaining sample indices:  $I_s \cup I_r = \{0, \dots, n_w - 1\}$ . Let us also define an activation function  $\Gamma(I, t)$  for a set of indices  $I$ :

$$\Gamma(I, t) = \begin{cases} 1 & \text{if } t \in \bigcup_{i \in I} [i \cdot T_s, (i+1) \cdot T_s[ \\ 0 & \text{otherwise} \end{cases} \quad (48)$$

The final state is a function  $g$  of the initial co-state given in (20). The integral in (19) results in two terms depending of the regular control and the singular control values, respectively:

$$g(\lambda_{\text{init}}) = h(\lambda_{\text{init}}) + Q^{-1} \int_0^T \psi_P(w, \lambda_{\text{init}}) \cdot \psi_\vartheta(w, \lambda_{\text{init}}) \cdot \Gamma(I_s, t) \cdot dt \quad (49)$$

where  $h(\lambda_{\text{init}})$  is the function that only depends on the regular control values:

$$h(\lambda_{\text{init}}) = x(0) + Q^{-1} \sum_{i \in I_r} \psi_P(w_i, \lambda_{\text{init}}) \cdot \psi_\vartheta(w_i, \lambda_{\text{init}}) \cdot s - Q^{-1} \sum_{i=0}^{n_w-2} w_i \cdot s \quad (50)$$

For a given final  $x_T$  value, an infinite number of optimal state trajectories can be obtained. They all correspond to the same total fuel consumption and are characterized by the following

additional optimality conditions:

$$Q^{-1} \int_0^T \psi_P(w, \lambda_{\text{init}}) \cdot \psi_\vartheta(w, \lambda_{\text{init}}) \cdot \Gamma(I_s, t) \cdot dt = x_T - h(\lambda_{\text{init}}) \quad (51)$$

Depending on the value of  $x_T$ , either the binary or continuous control can be singular for some  $i \in I_s$ .

Over any singular arcs, Pontryagin's Minimum Principle optimality conditions are satisfied by many different control signals. Let us define the two following control signals with feasible binary control ( $\vartheta_a(t) \in \{0, 1\}$  and  $\vartheta_b(t) \in \{0, 1\}$ ):

$$(\vartheta_a(t), P_a(t)) = (\max(\psi_\vartheta(w, \lambda_{\text{init}}), \max(\psi_P(w, \lambda_{\text{init}}))) \quad (52)$$

$$(\vartheta_b(t), P_b(t)) = (\min(\psi_\vartheta(w, \lambda_{\text{init}}), \min(\psi_P(w, \lambda_{\text{init}}))) \quad (53)$$

When the control is singular,  $\vartheta_a(t) \cdot P_a(t)$  (resp.  $\vartheta_b(t) \cdot P_b(t)$ ) corresponds to the maximum (resp. minimum) of the optimal power that can be produced by the auxiliary power unit.

When the control is not singular, the two control signals are equal:

$$(\vartheta_a(t), P_a(t)) = (\vartheta_b(t), P_b(t)) \quad \forall t / \Gamma(I_R, t) = 1 \quad (54)$$

Using the two control signals  $(\vartheta_a(t), P_a(t))$  and  $(\vartheta_b(t), P_b(t))$ , two state trajectories  $x_a$  and  $x_b$  are obtained. The final state values  $x_a(T)$  and  $x_b(T)$  correspond to maximum and minimum final state values reachable with the initial co-state value  $\lambda_{\text{init}}$  as depicted in Fig. 13. For  $x_0 = 50\%$  and  $x_T = 45.79\%$ , the initial co-state to be used is  $\lambda_{\text{init}} = -Qc_5 = -2087.53$ . This corresponds to state trajectories with a possible singularity of the continuous variable  $P$ . The binary variable  $\vartheta$  is always regular. Due to saturation, the continuous control can be singular when the exogenous variable  $w$  is above 10 kW: during vehicle acceleration phases (for instance  $\forall t \in [566, 574]$ ) or during the high speed driving phase (for instance  $\forall t \in [1072, 1157]$ ). When the continuous control  $P$  is singular, the admissible control values depend on the lookup table breakpoints  $\{p_5 = 17.8 \text{ kW}, p_6 = 22.2 \text{ kW}\}$  and the control constraint (5):

$$P(t) \in [\max(p^5, \underline{P}(w)), \min(p^6, \bar{P}(w))] \quad (55)$$

As a result, final state variations as large as  $x_a - x_b = 2.7\%$  can be obtained due to singular control.

### C. Proposed Algorithm

Let us consider only the optimal solutions obtained by switching between the control signals  $(\vartheta_a(t), P_a(t))$  and  $(\vartheta_b(t), P_b(t))$ . Using  $(\vartheta_b(t), P_b(t)) \quad \forall t \in [0, T]$  does not allow the auxiliary power unit to produce enough energy as  $x_b(T) < x_T$ . The additional amount of energy to be generated using the control law  $(\vartheta_a(t), P_a(t))$  is  $x_T - x_b(T)$ . The

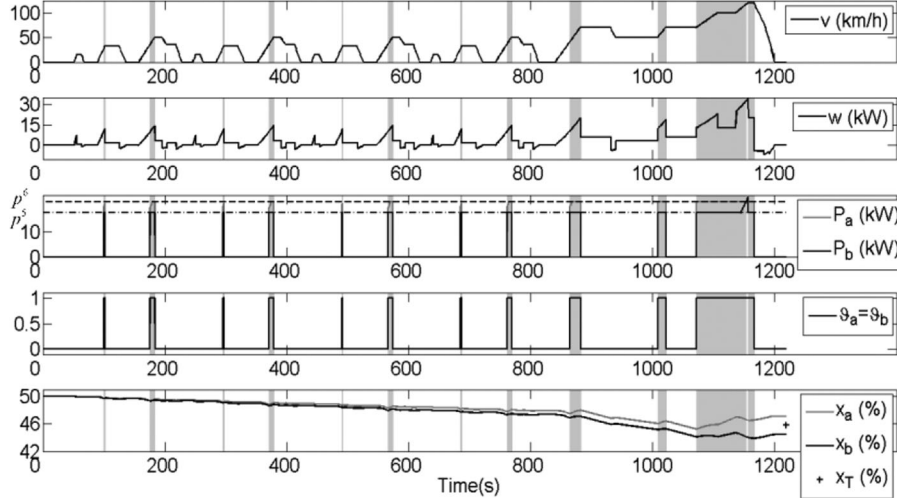


Fig. 13. Example of a singular continuous variable obtained with the NEDC for  $\lambda_{\text{init}} = -Qc_5 = -2087.53$ . Grayed areas correspond to singular control.

additional optimality condition (51) can be reformulated:

$$\int_0^T Q^{-1} (\vartheta(t) \cdot P(t) - \vartheta_b(t) \cdot P_b(t)) \cdot \Gamma(I_s, t) \cdot dt = x_T - x_b(T) \quad (56)$$

In practice, it is often preferred to limit the number of switches, especially for the binary control signal. Let us consider the control signals composed of maximum two switches between  $(\vartheta_a(t), P_a(t))$  and  $(\vartheta_b(t), P_b(t))$ . By introducing two additional control parameters  $t_{\text{min}}, t_{\text{max}} \in [0, T]$  such that  $t_{\text{max}} > t_{\text{min}}$ , the proposed control law is:

$$(\vartheta, P) = \begin{cases} (\vartheta_a, P_a) & \text{if } t \geq t_{\text{min}} \text{ and } t \leq t_{\text{max}} \\ (\vartheta_b, P_b) & \text{otherwise} \end{cases} \quad (57)$$

Additional dynamics are used to evaluate the amount of energy produced using  $(\vartheta_a(t), P_a(t))$ :

$$\dot{\sigma}(t) = \begin{cases} \frac{(\vartheta_a(t)P_a(t) - \vartheta_b(t)P_b(t))\Gamma(I_s, t)}{Q} & \forall t \geq t_{\text{min}} \\ 0 & \text{otherwise} \end{cases} \quad (58)$$

With  $\sigma(0) = 0$ . The proposed control law can be rewritten:

$$(\vartheta, P) = \begin{cases} (\vartheta_a, P_a) & \text{if } t \geq t_{\text{min}} \text{ and } \sigma(t) < x_T - x_b(T) \\ (\vartheta_b, P_b) & \text{otherwise} \end{cases} \quad (59)$$

The derivation of the optimal control problem solution is reduced to the computation of the switching time  $t_{\text{max}}$ :

$$\sigma(t_{\text{max}}) = x_T - x_b(T) \quad (60)$$

There is always a solution for  $t_{\text{min}} = 0$ . Other  $t_{\text{min}}$  values may be used to generate other optimal solutions.

Let us note that  $(\vartheta_a(t), P_a(t))$  and  $(\vartheta_b(t), P_b(t))$  are piecewise constant signals. Let us denote by  $\vartheta_{a,i}, P_{a,i}, \vartheta_{b,i}$  and  $P_{b,i}$

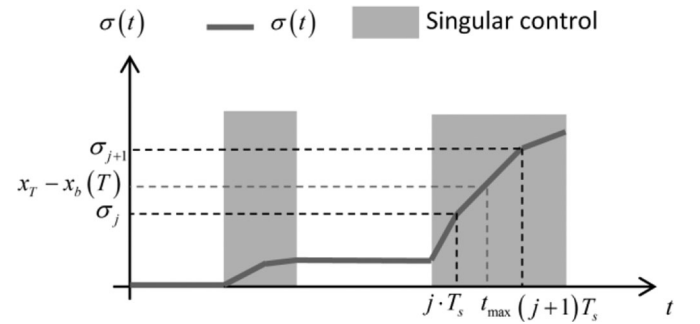


Fig. 14. Computation of  $t_{\text{max}}$ , the switching time from  $(\vartheta_a(t), P_a(t))$  to  $(\vartheta_b(t), P_b(t))$ .

the control values over the time interval  $[iT_s, (i+1)T_s[$ :

$$\begin{cases} \vartheta_a(t) = \vartheta_{a,i} \\ P_a(t) = P_{a,i} \end{cases} \quad \forall t \in [iT_s, (i+1)T_s[ \quad (61)$$

$$\begin{cases} \vartheta_b(t) = \vartheta_{b,i} \\ P_b(t) = P_{b,i} \end{cases} \quad \forall t \in [iT_s, (i+1)T_s[ \quad (62)$$

For the sake of simplicity, let us choose  $t_{\text{min}} = 0$ .  $\sigma$  is a piecewise linear signal:

$$\sigma(t) = \alpha_i(t - t_i) + \sigma_i \quad \forall t \in [iT_s, (i+1)T_s[ \quad (63)$$

Where  $\sigma_{i+1} = \alpha_i T_s + \sigma_i$ ,  $\sigma_0 = 0$  and  $\alpha_i = Q^{-1}((\vartheta_{a,i} \cdot P_{a,i} - \vartheta_{b,i} \cdot P_{b,i}) \cdot \Gamma(I_s, i \cdot T_s))$ .

As  $\vartheta_{a,i} \cdot P_{a,i} \geq \vartheta_{b,i} \cdot P_{b,i}$ ,  $\sigma(t)$  is a monotonic increasing function of time. To compute the switching time between  $(\vartheta_a(t), P_a(t))$  and  $(\vartheta_b(t), P_b(t))$ , it is suggested to compute the  $\sigma_i$  values, starting from  $i = 0$ , until the desired value  $x_T - x_b(T)$  is reached over a sampling period. Let us denote  $j$  as the sample index such that:

$$\sigma_j < x_T - x_b(T) < \sigma_{j+1} \quad (64)$$

Once the proper  $j$  value is obtained the derivation of  $t_{\max}$  is straightforward, as illustrated in Fig. 14.

$$t_{\max} = (x_T - x_b(T) - \sigma_j) \alpha_j^{-1} + t_j \quad (65)$$

In general, the  $t_{\max}$  obtained is not a multiple of the driving cycle sampling period  $T_s$ .

Finally, for  $t_{\min} = 0$  the control algorithm is obtained as follows:

- 1) Compute the sets  $\Omega_v$  and  $\Omega_\vartheta$  of initial co-state values that lead to singular variables.
- 2) Using a bisection search algorithm within the ordered set  $\Omega$ , search for  $\lambda_{\text{init}}$  such that  $\min(g(\lambda_{\text{init}})) < x_T < \max(g(\lambda_{\text{init}}))$ .
- 3) Compute the two control signals  $(\vartheta_a(t), P_a(t))$  and  $(\vartheta_b(t), P_b(t))$  for all  $t \in [0, T]$  and their corresponding state trajectories  $x_a$  and  $x_b$ .
- 4) Starting from  $j = 0$ , compute  $\sigma_{j+1}$  until condition (64) is met. Compute the switching time  $t_{\max}$  using (65).
- 5) Using the piecewise constant optimal control (59), compute the optimal state trajectory using the state dynamics given by (6).

Other optimal state trajectories can be obtained by modifying  $t_{\min}$ . Whatever the value of  $t_{\min}$ ,  $\sigma(t)$  is still a monotonic increasing piecewise linear signal. If  $t_{\min}$  is a multiple of the sampling period  $T_s$ , it is sufficient to use a modified  $\alpha_i$  in (63):

$$\alpha_i = Q^{-1} ((\vartheta(i \cdot T_s) \cdot P(i \cdot T_s) - \vartheta_{b,i} \cdot P_{b,i}) \cdot \Gamma(I_s, i \cdot T_s)) \quad (66)$$

The proposed approach is still valid if  $t_{\min}$  is not a multiple of the sampling period, but a more tedious implementation is required to account for the initial control law switching time when computing  $\sigma(t)$  using (58).

## V. SIMULATION RESULTS

Two use cases were studied. The first one corresponds to the series hybrid vehicle used to present the optimal control law derivation. The second one corresponds to the parallel hybrid vehicle introduced in Section II. From the simulation results and the previous theoretical study, the main factors influencing the occurrence of the numerical errors encountered are highlighted. Then, practical recommendations for engineers are provided in Section V-C.

### A. Series Hybrid Vehicle

Two optimal control signals have been generated for the NEDC for  $x_T = 45.79\%$ . To obtain this final state value, the initial co-state value is  $\lambda_{\text{init}} = -Qc_5 = -2087.53$ . The continuous variable  $P$  is singular over some time intervals, whereas the binary variable is always regular. The control signal and state trajectories obtained are presented in Fig. 15. The first control signal corresponds to  $t_{\min} = 0$  s and  $t_{\max} = 1082.89$  s. The second one corresponds to  $t_{\min} = 1083$  s and  $t_{\max} = 1165.11$  s. The two corresponding state trajectories end exactly at  $x_T = 45.79\%$  (the actual final state deviation  $|x(T) - x_T|$  is lower than  $10^{-13}\%$  due to numerical implementation). The fuel consumption is identical for both (3.54 l/100 km). The dynamic

TABLE IV  
OPTIMAL FUEL CONSUMPTION OVER THE SELECTED DRIVING CYCLES, SERIES HYBRID VASE

Driving cycle	Final state of charge $x_T$ (%)	$t_{\max}$ (s)	Fuel consumption (l/100 km/h)
NEDC	85.67	430.00	3.90
HYZEM Urban	63.18	113.00	5.99
HYZEM Road	50.21	476.94	6.32
HYZEM Highway	42.90	800.95	6.85

programming (DP) algorithm has also been used to compute a solution [30]. It is denoted as “DP” in the Fig. 15. The state quantification step is chosen as 100 J. The obtained fuel consumption is 3.57 l/100 km. Due to the state quantification, the DP solution results in a higher fuel consumption (+0.03 l/100 km). Moreover, the computation time was 490 s compared to 2.64 ms required by the proposed control law.

The deviations between both control signals and state trajectories are quite small. The admissible control variation is limited by (i) the control saturation and (ii) the difference between the two lookup table breakpoints:  $p_6 - p_5 = 4.44$  kW.

The proposed control law was applied to the other driving cycles considered for the final state of charge given in Table III. The results are summarized in Table IV. The proposed control algorithm was applied with  $x_0 = 50\%$  and  $t_{\min} = 0$ s. The final state of charge is reached exactly (the largest final state error is  $6 \cdot 10^{-12}\%$ ).

In addition to the optimal control signal behavior analysis, the algorithm implementation is discussed next. Interpolation is the most time-consuming operation. The control law proposed can be implemented very efficiently; it only requires a few interpolations to compute the minimum and maximum control values  $\underline{P}(w_i)$  and  $\bar{P}(w_i)$ . The remaining computations do not need any additional interpolation. In the classical implementation of Pontryagin’s Minimum Principle, the fuel consumption is computed using one interpolation for every value in  $U_{\text{grid}}$ , which is a large set (732 000 values for the simulation presented).

Both algorithms require a bisection search to find the initial co-state value. For the algorithm proposed, the bisection search is restricted to an ordered set of possible initial co-state values  $\Omega$ . As this set is finite, the number of bisection iterations is also finite. It only depends on the driving cycle length and the number of lookup table breakpoints. With the classical implementation of Pontryagin’s Minimum Principle, the number of bisection iterations is unlimited. For the series hybrid vehicle chosen, it is proven that the final state value can only be reached if singular control is considered. As a result, the execution time depends mostly on the maximum number of iterations allowed.

The algorithm proposed and the classical implementation of Pontryagin’s Minimum Principle were executed on an Intel Core i7-3520 [12] M 2.9 GHz laptop computer with 4 Gb of RAM running Windows 7. The algorithms were implemented using MATLAB and both codes were optimized using vectorization techniques. The native “interp1” function was used for the linear interpolations. The computation task consisted in computing an optimal state trajectory for 50 different  $x_T$  values over the NEDC. To improve accuracy, this task was executed 20 times

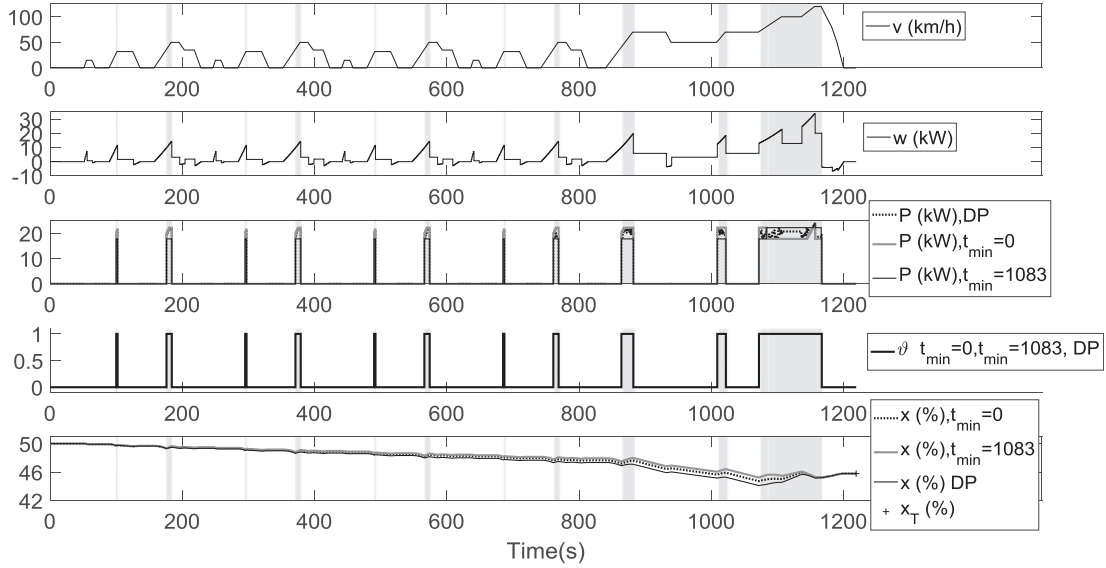


Fig. 15. Dynamic programming result and two optimal control solutions with a singular continuous variable obtained using  $t_{\min} = 0$  s and  $t_{\min} = 1083$  s. Grayed areas correspond to singular control.

TABLE V  
AVERAGE EXECUTION TIMES OF THE PROPOSED ALGORITHM AND THE CLASSICAL IMPLEMENTATION OF PONTRYAGIN'S MINIMUM PRINCIPLE

Algorithm	Maximum number of bisection iterations	Average execution time
Classical PMP implementation	50	45.7 ms
	100	69.8 ms
	200	114 ms
Proposed control law	142	2.64 ms

TABLE VI  
OPTIMAL FUEL CONSUMPTION OVER THE SELECTED DRIVING CYCLES FOR THE PARALLEL HYBRID VEHICLE

Driving cycle	Initial state of charge $x_0$ (%)	Expected final state of charge $x_T$ (%)	$t_{\max}$ (s)	Fuel consumption (l/100 km)
NEDC	50	67.15	981.00	4.80
HYZEM Urban	50	60.45	61.50	5.14
HYZEM Road	50	70.25	192.00	4.45
HYZEM Highway	100	6.62	1545.00	4.45

and the average execution time for a single optimal trajectory was obtained. The results are provided in Table V. As expected, the proposed algorithm is significantly faster (at least seventeen times) than the classical one. Similar improvements were tested when deriving a similar optimal control algorithm for other arrangements such as a parallel single shaft.

### B. Parallel Single Shaft Vehicle

The optimal control problem in the case of a parallel single shaft algorithm is similar to the optimal control problem (4), (6), (9)–(11) except that the lookup table parameters are time dependent. Consequently, the number of co-state values that leads to singular control is significantly higher and the effect on the final state of charge error is potentially lower.

The optimal control algorithm was applied to the NEDC. The simulation parameters were  $x_0 = x_T = 50\%$  and the optimal solution was computed for  $t_{\min} = 0$  s. The initial co-state obtained is  $\lambda(0) = -5.63 \cdot 10^2$  and induces singular binary control. The final state of charge was reached exactly (up to a numerical error of  $|x(T) - x_T| = 2.55 \cdot 10^{-13}\%$ ). The corresponding fuel consumption was 3.59 l/100 km.

Simulations were also conducted with the other driving cycles and the simulation parameters corresponding to the worst cases given in Table II. For the HYZEM Highway, the simulation conditions also correspond to a deep battery discharge whereas for the other driving cycles the battery was recharged. For each driving cycle, the optimal control algorithm proposed computes the value of the  $t_{\max}$  parameter so the final state of charge is reached exactly. For all the driving cycles considered, the final state of charge error was lower than  $5.55 \cdot 10^{-13}\%$ .

### C. Discussion

Singular control can induce final state of charge errors. Depending on the architecture and the driving cycle, these errors may be higher or lower. Four factors can be highlighted.

*Vehicle architecture.* Series hybrid vehicles have a fuel consumption that does not depend on any parameters other than control. As a result, the cumulated length of singular arcs can be substantial. This is clearly visible in Fig. 15 where a significant share of the driving cycle samples leads to singular control. For some architectures such as the parallel hybrid vehicle, the fuel consumption model depends on the IC engine shaft speed. So, for a given co-state, only the samples that correspond to the same IC engine rotation speed can be singular and the cumulated effect of the singular control is less important.

*Fuel consumption model.* Using linear interpolation with a lookup table to model the fuel consumption leads to singular control. The overall final state of charge error depends mostly on the number of vertices (for equally sampled breakpoints). In

practice, with maps containing more than 20 vertices, the final state of charge error remains quite small.

*Binary (and/or integer) signal optimization.* Optimizing the IC engine ‘on/off’ signal induces singular control for all the hybrid vehicles, regardless of their mechanical and electrical structure. The same issue is encountered with clutches when their open/close state is optimized. For the series and parallel hybrid vehicles studied, when the IC engine on/off control signal is singular, the optimality condition requires the continuous signal to be set so as to maximize powertrain efficiency. In practice, the best efficiency is reached for high torque/power values and so the overall effect on the final state of charge can be significant (one must decide to switch the primary source off or to generate a high power/torque).

*Driving cycle.* From the authors’ experience, for most of the hybrid vehicles, singular control over the NEDC always has a significant influence on the final state of charge. This is due to the repetitive patterns used to build this driving cycle. Singular control is repeated with the velocity patterns used to build this driving cycle and thus its effects are cumulated in the final state of charge.

From the theoretical study proposed, two recommendations and explanations can be formulated for a wide variety of hybrid vehicles.

*Boundary Value Problem solvers will not work if a binary variable is optimized.* When programming optimal hybrid vehicle energy management, one of the difficulties is computing the initial co-state  $\lambda_{\text{init}}$  so the expected final state is reached. Actually, the initial co-state  $\lambda_{\text{init}}$  is the only unknown in the following two-point boundary value problem (BVP):

$$\dot{x} = (\psi_P(w, \lambda) \cdot \psi_\theta(w, \lambda) - w(t)) Q^{-1} \quad (67)$$

$$\dot{\lambda} = 0 \quad (68)$$

$$x(0) = x_0, x(T) = x_T \quad (69)$$

BVP solvers based on a collocation algorithm (e.g., BVP4C solver in MATLAB) require the right hand side of the differential equation (67)–(68) to be smooth enough. The optimal control given by (43)–(44) and depicted in Fig. 12 is clearly discontinuous. This explains why it is not possible to use collocation-based solvers to solve optimal hybrid vehicle energy management with binary variable optimization. Differential equations (67)–(68) are marginally stable, therefore, the shooting method proposed should be preferred. Problems without binary variable optimization can be solved with a collocation-based solver if the fuel consumption is modeled using a function which has a continuous first derivative (e.g., spline).

*Root-finding algorithm.* A root-finding algorithm is used to numerically compute a solution of  $g(\lambda_{\text{init}}) = x_T$ . When singular control occurs, the function  $g$  is discontinuous, Fig. 8. In the vicinity of a discontinuity of the  $g$  function, gradient-based root-finding algorithms (e.g., Newton’s method) are not likely to perform well, since the derivative of  $g$  is undefined. Instead, bracketing methods (e.g., bisection method) are preferable. At each iteration  $i$ , these algorithms compute  $\bar{\lambda}_i$  and  $\underline{\lambda}_i$ , an upper and a lower bound of the unknown solution  $\lambda_{\text{init}}$  such that  $\lambda_{\text{init}} \in [\underline{\lambda}_i, \bar{\lambda}_i]$ . If no singular control occurs, each iteration im-

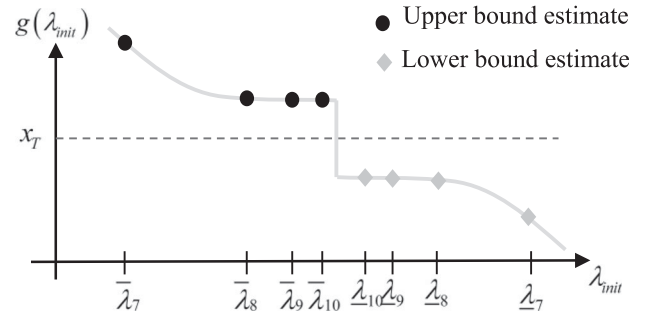


Fig. 16. Non convergence of the root-finding algorithm.

proves the accuracy of the estimation:  $\bar{\lambda}_{i-1} - \underline{\lambda}_{i-1} > \bar{\lambda}_i - \underline{\lambda}_i$  and convergence is ensured. Ultimately,  $\bar{\lambda}_{i-1} - \underline{\lambda}_{i-1} \rightarrow 0$  and  $g(\bar{\lambda}_i) = g(\underline{\lambda}_i) = x_T$  when  $i \rightarrow +\infty$ . Fig. 16 depicts the situation when singular control occurs. The function  $g$  is discontinuous. It is quite easy to detect this situation by analyzing the successive values of the upper and lower bounds:  $\bar{\lambda}_i$  and  $\underline{\lambda}_i$  converge toward  $\lambda_{\text{init}}$  but  $g(\bar{\lambda}_i) - g(\underline{\lambda}_i)$  converges toward a non-null value.

## VI. CONCLUSION

Linear interpolations between lookup table data and binary control signals can induce multiple Hamiltonian minima and therefore lead to multiple optimal trajectories. The construction of optimal trajectories with a singular control signal has been analyzed and discussed. The main idea is that singular control actions should be chosen appropriately such that a specific amount of energy is produced over the entire driving cycle. This provides numerous possibilities for generating multiple optimal state trajectories.

A simple control strategy, described as mathematical algorithms, has been proposed. It consists in switching the control signal between its minimum and maximum admissible values to reach the final state value defined.

The proposed algorithm is very efficient (17 times faster than the classical implementation of Pontryagin’s Minimum Principle) and can be easily extended to other hybrid vehicle arrangements and perform gear shift optimization. Finally, future work will be devoted to limiting the frequency of the binary variable switches to cope with the practical limits of the auxiliary power unit.

## APPENDIX VEHICLE MODELING

A simplified model is considered. Using the vehicle dynamics and the vehicle parameters, as defined in Table VII, the power at the wheel  $P_w$  produced by the powertrain on a flat road is computed using:

$$P_w(t) = \frac{1}{2} \cdot \rho_{\text{air}} A_f c_d \rho_{\text{air}} v(t)^3 + M v(t) \left( g_{crr} + \frac{dv(t)}{dt} \right) \quad (70)$$

Considering that only 40% of the vehicle’s kinetic energy can be recovered and  $\eta_{em}$  a constant electric machine efficiency, the

TABLE VII  
MODEL PARAMETERS

Description	Value
Air density	$\rho_{air} = 1.225 \text{ kg} \times \text{m}^{-3}$
Vehicle frontal area	$A_f = 1.9 \text{ m}^2$
Drag coefficient	$C_d = 0.28$
Vehicle mass	$M = 1200 \text{ kg}$
Gravity acceleration	$g = 9.81 \text{ ms}^{-2}$
Rolling resistance coefficient	$c_{rr} = 0.01$
Electric machine average efficiency	$\eta_{em} = 0.8$
Auxiliary power unit maximum power	$P_{max}^{apu} = 40 \text{ kW}$
Power that leads to best APU efficiency	$P_{be} = 22 \text{ kW}$
Energy storage system capacity	$Q = 24.84 \text{ MJ}$
Energy storage system maximum power	$y_{max}^e = 10 \text{ kW}$

driving cycle power  $w(t)$  is obtained:

$$w(t) = \begin{cases} P_w(t) \cdot \eta_{em}^{-1} & \text{if } P_w(t) > 0 \\ P_w(t) \cdot \eta_{em} \cdot 0.4 & \text{otherwise} \end{cases} \quad (71)$$

#### REFERENCES

- [1] T. J. Böhme and B. Frank, *Hybrid Systems, Optimal Control and Hybrid Vehicles*. New York, NY, USA: Springer, 2017.
- [2] X. Meng and N. Langlois, "Optimized fuzzy logic control strategy of hybrid vehicles using ADVISOR," in *Proc. 2010 Int. Conf. Comput., Mechatronics, Control Electron. Eng.*, 2010, pp. 444–447.
- [3] W. Aiguo, "Research on optimal control of hybrid vehicle torque distribution," in *Proc. 12th Int. Comput. Conf. Wavelet Active Media Technol. Inf. Process.*, 2015, pp. 476–481.
- [4] D. J. van Mullem, T. A. C. van Keulen, J. T. B. A. Kessels, B. de Jager, and M. Steinbuch, "Implementation of an optimal control energy management strategy in a hybrid truck," in *Proc. Adv. Automotive Control*, Schwabing, Germany, 2013, pp. 61–66.
- [5] S. Delprat, J. Lauber, T. M. Guerra, and J. Rimaux, "Control of a parallel hybrid powertrain: Optimal control," *IEEE Trans. Veh. Technol.*, vol. 53, no. 3, pp. 872–881, May 2004.
- [6] E. Tazelaar, Y. Shen, P. A. Veenhuizen, T. Hofman, and P. P. J. van den Bosch, "Sizing stack and battery of a fuel cell hybrid distribution truck," *Oil Gas Sci. Technol.*, vol. 67, no. 4, pp. 563–573, 2012.
- [7] S. Kermani, S. Delprat, T. M. Guerra, R. Trigui, and B. Jeanneret, "Predictive energy management for hybrid vehicle," *Control Eng. Pract.*, vol. 20, no. 4, pp. 408–420, Apr. 2012.
- [8] P. Elbert, T. Nuesch, A. Ritter, N. Murgovski, and L. Guzzella, "Engine on/off control for the energy management of a serial hybrid electric bus via convex optimization," *IEEE Trans. Veh. Technol.*, vol. 63, no. 8, pp. 3549–3559, Jan. 2014.
- [9] L. Guzzella and A. Sciarretta, *Vehicle Propulsion Systems: Introduction to Modeling and Optimization*. New York, NY, USA: Springer-Verlag, 2005.
- [10] L. V. Pérez, C. H. de Angelo, and V. Pereyra, "Determination of the adjoint state evolution for the efficient operation of a hybrid electric vehicle," *Math. Comput. Model.*, vol. 57, no. 9–10, pp. 2257–2266, May 2013.
- [11] F. Payri, C. Guardiola, B. Pla, and D. Blanco-Rodríguez, "A stochastic method for the energy management in hybrid electric vehicles," *Control Eng. Pract.*, vol. 29, pp. 257–265, Aug. 2014.
- [12] T. van Keulen, "Fuel optimal control of hybrid vehicle," Ph.D. dissertation, Technische Universiteit Eindhoven, Eindhoven, The Netherlands, 2011.
- [13] E. Vinot and R. Trigui, "Optimal energy management of HEVs with hybrid storage system," *Energy Convers. Manage.*, vol. 76, pp. 437–452, Dec. 2013.
- [14] T. Nüesch, P. Elbert, M. Flankl, C. Onder, and L. Guzzella, "Convex optimization for the energy management of hybrid electric vehicles considering engine start and gearshift costs," *Energies*, vol. 7, no. 2, pp. 834–856, Feb. 2014.
- [15] S. Ebbesen, M. Salazar, P. Elbert, C. Bussi, and C. H. Onder, "Time-optimal control strategies for a hybrid electric race car," *IEEE Trans. Control Syst. Technol.*, no. 99, pp. 1–15, 2017.

- [16] M. C. Grant and S. P. Boyd, "Graph implementations for nonsmooth convex programs," in *Recent Advances in Learning and Control, Lecture Notes in Control and Information Sciences*, V. Blondel, S. Boyd, and H. Kimura, Eds. London, U.K.: Springer-Verlag, 2008, pp. 95–110.
- [17] W. Rui and S. M. Lukic, "Dynamic programming technique in hybrid electric vehicle optimization," in *Proc. 2012 IEEE Int. Elect. Veh. Conf.*, 2012, pp. 1–8.
- [18] O. Sundström, D. Ambühl, and L. Guzzella, "On implementation of dynamic programming for optimal control problems with final state constraints," *Oil Gas Sci. Technol.*, vol. 65, no. 1, pp. 91–102, Sep. 2010.
- [19] Z. Yuan, L. Teng, S. Fengchun, and H. Peng, "Comparative study of dynamic programming and Pontryagin's minimum principle on energy management for a parallel hybrid electric vehicle," *Energies*, vol. 6, no. 4, pp. 2305–2318, Apr. 2013.
- [20] R. F. Hartl, S. P. Sethi, and R. G. Vickson, "A survey of the maximum principles for optimal control problems with state constraints," *SIAM Rev.*, vol. 37, no. 2, pp. 181–218, Jun. 1995.
- [21] T. van Keulen, J. Gillot, B. de Jager, and M. Steinbuch, "Solution for state constrained optimal control problems applied to power split control for hybrid vehicles," *Automatica*, vol. 50, no. 1, pp. 187–192, Jan. 2014.
- [22] G. Rousseau, "Véhicule hybride et commande optimale," Ph.D. dissertation, Ecole des Mines de Paris, Paris, France, 2008.
- [23] S. Stockar, V. Marano, M. Canova, G. Rizzoni, and L. Guzzella, "Energy-optimal control of plug-in hybrid electric vehicles for real-world driving cycles," *IEEE Trans. Veh. Technol.*, vol. 60, no. 7, pp. 2949–2962, Jun. 2011.
- [24] D. E. Kirk, *Optimal Control Theory: An Introduction*. Mineola NY, USA: Dover, 2004.
- [25] H. Schättler and U. Ledzewicz, "The Pontryagin maximum principle: From necessary conditions to the construction of an optimal solution," in *Geometric Optimal Control*. New York, NY, USA: Springer-Verlag, 2012, pp. 83–194.
- [26] N. Murgovski, L. Johannesson, J. Sjöberg, and B. Egardt, "Component sizing of a plug-in hybrid electric powertrain via convex optimization," *Mechatronics*, vol. 22, no. 1, pp. 106–120, Feb. 2012.
- [27] T. van Keulen, D. van Mullem, B. de Jager, J. T. B. A. Kessels, and M. Steinbuch, "Design, implementation, and experimental validation of optimal power split control for hybrid electric trucks," *Control Eng. Pract.*, vol. 20, no. 5, pp. 547–558, May 2012.
- [28] C. Hou, M. Ouyang, L. Xu, and H. Wang, "Approximate Pontryagin's minimum principle applied to the energy management of plug-in hybrid electric vehicles," *Appl. Energy*, vol. 115, pp. 174–189, Jan. 2014.
- [29] P. Riedinger, J. Daafouz, and C. Iung, "Suboptimal switched controls in context of singular arcs," in *Proc. 42nd IEEE Conf. Decis. Control*, 2003, pp. 6254–6259.
- [30] V. Larsson, L. Johannesson, and B. Egardt, "Analytic solutions to the dynamic programming subproblem in hybrid vehicle energy management," *IEEE Trans. Veh. Technol.*, vol. 64, no. 4, pp. 1458–1467, Apr. 2015.



**Sébastien Delprat** received the Ph.D. degree in 2002 from the University of Valenciennes and Hainaut Cambresis, Valenciennes, France, where he became an Assistant Professor. Since 2012, he has been a Full Professor. His research interests include vehicle control, and especially hybrid vehicle energy management.



**Theo Hofman** received the M.Sc. (with Hons.) and Ph.D. degrees in mechanical engineering from the Eindhoven University of Technology, Eindhoven, The Netherlands, in 1999 and 2007, respectively. From 1999 to 2003, he was a researcher and the Project Leader with Thales-Cryogenics. Since 2009, he has been an Assistant Professor in the Control Systems Technology Group, Department of Mechanical Engineering, Eindhoven University of Technology. His research interests include the modeling, design, and control of hybrid propulsion systems.

Sébastien Paganelli, photograph and biography not available at the time of publication.